*International Journal of Neuropsychopharmacology* (2011), **14**, 535–544. © CINP 2010
doi:10.1017/S1461145710000891

ARTICLE

CINP

# Characterization of electroconvulsive seizure-induced TIMP-1 and MMP-9 in hippocampal vasculature

**Matthew J. Girgenti, Emily Collier, Monica Sathyanesan, Xiaowei W. Su and Samuel S. Newton**

*Division of Molecular Psychiatry, Abraham Ribicoff Research Facilities, Connecticut Mental Health Center, Yale University School of Medicine, New Haven, CT, USA*

**Abstract**

Degradation of the vascular basement membrane stimulates angiogenesis and is tightly controlled by balancing the actions of metalloproteases and their inhibitors. Previous work demonstrated that electroconvulsive seizure (ECS) elevates angiogenic factors and endothelial proliferation in the hippocampus. The robust induction of tissue inhibitor of matrix metalloprotease 1 (TIMP-1) in the stratum lacunosum moleculare (SLM) corresponds to sites of increased vascular density. This led us to examine the spatial and cellular expression of TIMP-1 and its substrate, matrix metalloprotease 9 (MMP-9). Chronic ECS increased TIMP-1 by 12-fold and MMP-9 by 3-fold in discrete SLM cells. We then characterized the expression of TIMP-1 mRNA in relation to vasculature in the SLM and glial-limiting membrane (GLM). Employing laser microdissection we identified the cell types associated with SLM vasculature and also phenotyped the cells expressing TIMP-1 and MMP-9. We concluded that TIMP-1 is produced by perivascular cells positive for alpha smooth actin and that MMP-9 is expressed by GFAP-positive astrocytes. These studies suggest that ECS-induced remodelling occurs at the vascular basement membrane and facilitates neovascularization.

*Received 10 November 2009; Reviewed 16 December 2009; Revised 4 June 2010; Accepted 6 July 2010; First published online 3 August 2010*

**Key words**: Antidepressant, angiogenesis, blood vessel, gene expression, metalloprotease.

## Introduction

Electroconvulsive seizure (ECS) is a therapeutically effective non-chemical antidepressant treatment that is frequently employed in severe depression and cases resistant to chemical antidepressants. Although significant progress has been made in identifying genes (Altar *et al.* 2004) and cellular processes (Madsen *et al.* 2000) induced by ECS, a clear understanding of its mechanism of action is not yet available. The regulation of neurotrophic (Nibuya *et al.* 1995), angiogenic (Newton *et al.* 2003) and trophic signalling molecules (Newton *et al.* 2004) have been demonstrated by *in-situ* hybridization and microarray studies, suggesting that the elevation of trophic factor-signalling cascades might constitute an important component of ECS-induced molecular effects. The increase in trophic factor gene expression appears to also have robust cellular consequences as increases in adult hippocampal neurogenesis (Madsen *et al.* 2000; Malberg *et al.* 2000) and endothelial proliferation (Hellsten *et al.* 2004) has been convincingly reported.

Recent studies have shown that the ECS-induced increase in endothelial proliferation results in enhanced hippocampal vascular density (Hellsten *et al.* 2005; Newton *et al.* 2006), raising the possibility that ECS has significant effects on cerebral vasculature that could contribute to its therapeutic efficacy. Previously, we showed that gene expression of tissue inhibitor of matrix metalloprotease 1 (TIMP-1) shifted from a predominant elevation in the dentate gyrus after acute ECS, to high levels in the stratum lacunosum moleculare (SLM) after chronic ECS (Newton *et al.* 2003). The SLM also exhibits a robust increase in angiogenesis. The striking elevation in TIMP-1 indicated that matrix metalloproteases (MMPs) might be activated by ECS and participate in matrix remodelling. The importance of MMPs and TIMPs in modulating diverse

Address for correspondence: Dr S. S. Newton, 34 Park Street, New Haven, CT 06508, USA.
*Tel.*: (203) 974-7733 *Fax*: (203) 974-7897
*Email*: Samuel.Sathyanesan@yale.edu

physiological, pathological and regenerative (Zhao *et al.* 2006) processes led us to examine in detail the phenotype of cells expressing TIMP-1 and MMP-9 by immunohistochemical and immuno-*in situ* co-localization with astrocytic and vascular markers. We also tested the activity of MMPs by *in-situ* zymography and mRNA expression levels in hippocampal vasculature by laser microdissection followed by real-time PCR analysis. In addition, we analysed the expression of connective tissue growth factor (CTGF), a growth factor involved in angiogenesis and extracellular matrix remodelling.

## Materials and methods

### *Animals*

Male Sprague–Dawley rats (160–180 g; Charles River Laboratories, USA, were housed, four per cage, under standard illumination parameters (12-h light/dark cycle, lights on 07:00 hours) with food and water available *ad libitum*. Animal use procedures were in strict accordance with the National Institutes of Health Guide for the Care and Use of Laboratory Animals and were approved by the Yale University Animal Care and Use Committee. Animals were utilized in experiments after they reached a weight of 220 g.

### *ECS*

Rats were divided into two groups, ECS and control. Rats were placed in plastic cages containing fresh bedding before induction of seizures. Bilateral ECS was administered via moistened pads on spring-loaded ear-clip electrodes using a pulse generator (ECT Unit 57800–001; Ugo Basile, Italy) (frequency 100 pulses/s, pulse width 0.5 ms, shock duration 0.5 s, current 55 mA) (Madsen *et al.* 2000). This consistently produced a generalized grand mal seizure with characteristic clonic and tonic convulsions. ECS animals received 10 shocks over the 10-d period (one shock each day) and tissue was collected 6 h after the last seizure. Sham-treated animals were handled similar to ECS-treated animals and had ear-clips placed on their ears, but no shock was delivered. All animals were killed by swift decapitation. The brains were quickly removed and rapidly frozen on dry ice.

### In-situ *hybridization*

*In-situ* hybridization was performed using radiolabelled riboprobes according to conventional protocols with minor modifications (Newton *et al.* 2002). Riboprobes were generated by PCR amplification using gene-specific primers, CTGF: agcagctgggagaactgtgc, tccttgggctcatcacac; TIMP-1: gtgccccaacccaccccacag, gcacaccccacagccagcac. The reverse primer included a T7 template sequence (TAATACGACTCACTATAGGGAGA) on the 5′-end. Whole rat brain cDNA was used as the template for PCR, which was performed in a real-time PCR instrument (SmartCycler, USA) using the Quantitect Sybr Green PCR kit (Qiagen, USA). PCR product was purified by ethanol precipitation and was resuspended in TE buffer. One microgram of the 300-bp PCR product was used to produce radiolabelled riboprobe using a T7-based *in-vitro* transcription kit (Megashortscript, USA). All riboprobes were verified by sequencing of the PCR product. *In-situ* hybridization images were quantified using NIH Image software, and statistical analysis was performed using Microsoft Excel software.

### *Laser microdissection*

PEN-foil slides (Leica Microsystems, USA) were irradiated in a UV Stratalinker to preclude RNase contamination. Hippocampal cryocut sections (10 $\mu$m) from sham and ECS-treated rat brains were collected on PEN foil. Each slide was individually ethanol dehydrated and stained with Cresyl Violet to identify SLM cells that appeared to circumscribe vasculature. Laser microdissection was performed no more than 24 h after sectioning. Microdissection was performed on a Leica AS LMD (Leica Microsystems). Immediately following microdissection, samples were placed on dry ice and stored under refrigeration at $-80\ ^{\circ}$C until RNA purification and cDNA synthesis.

### *Single-cell microdissection*

A total of 40 individual Cresyl Violet-positive cells were cut from SLM ($n=3$) and processed for cDNA synthesis using the Cells-to-cDNA kit (see below). cDNA was precipitated with linear acrylamide and resuspended in 20 $\mu$l nuclease-free water. Four microlitres of the cDNA suspension was used for each PCR amplification reaction using gene-specific primers. cDNA of cells that were positive for TIMP-1 or MMP-9 were then tested for expression of vascular markers.

### *RNA isolation and cDNA synthesis*

RNA from laser microdissected cells was extracted using the Cells-to-cDNA kit according to the manufacturer's directions (Ambion, USA). The samples were reverse transcribed into cDNA using Oligo$(dT)_{18}$ primers provided by the manufacturer. cDNA was precipitated with linear acrylamide (Ambion) and resuspended in nuclease-free water for use in qRT–PCR.

### *qRT–PCR*

Gene specific primers were designed and tested for efficiency and specificity by serial dilutions and melt curve analysis. Sybr Green mix (Sigma, USA) was used to amplify cDNA. Real-time PCR (SmartCycler) analysis of laser microdissected cells was conducted. Primer sequences were GAPDH: ggtctacatgttccagtatgactct, gttgatgaccagcttcccattct; GFAP: acagacaggaggcggatgaa, ctcctcctccagcgactcaa; MMP-9: gcaaaccctgcgtatttcca, ccgagcgacctttagtggtg; PDGFr$\beta$: ttgccagctccaccttgaat, gtcgcaggagatggtggaag; PECAM: gactggcccctgtcacgtttc, cacggtttcttcgtggaagg; $\alpha$-SMA: gtcccagacaccagggagtg, ttggtgatgatgccgtgttc; TIMP-1: tcagccatcccttgcaaact, cgctctggtagcccttctca.

### *Immunohistochemistry*

Cryocut coronal sections (14 $\mu$m) were used for slide-based immunohistochemical analysis of protein expression according to Newton *et al.* (2002) with minor modifications. Sections were fixed in Histochoice fixative (Sigma) for 10 min followed by a 5-min wash in cold 1 × PBS. Slides were then immersed in 0.75% hydrogen peroxide (molecular biology grade, Sigma) in PBS for 5 min followed by two 5-min rinses in 1 × PBS. All incubations were performed on the slide by encircling sections with an ImmEdge pen (Vector Laboratories, USA), then adding liquid to the slide itself. Sections were blocked with 5.0% BSA (w/v) in PBS (molecular biology grade lyophilized BSA, Sigma) at 4 °C for 30 min. Sections were incubated with different primary antibody combinations in antibody solution (2.5% BSA in PBS) at 4 °C overnight [TIMP-1, 1:1000, R&D Systems (USA); MMP-9, 1:2000, Torrey Pines (USA); rat endothelial cell antigen (RECA), 1:50, Serotec (UK); GFAP (mouse), 1:3000, Millipore (USA)]. Following primary antibody incubation, slides were washed in 1 × PBS three times for 5 min each at room temperature. Slides were then incubated in fluorescent secondary antibody (1:1000, Alexa-488 and 594 conjugated donkey anti-mouse and donkey anti-rabbit secondary antibodies; Molecular Probe, USA) in 2.5% BSA in PBS for 2 h at room temperature. The slides were then rinsed in 1 × PBS three times for 5 min each and mounted wet using Gel Mount (USA) and coverslipped. Sections were imaged using a fluorescence microscope with appropriate filters.

### *Immuno*-in situ

Combined immunohistochemistry and *in-situ* hybridization followed by emulsion autoradiography was performed on cryocut sections based on protocols that were previously optimized in our laboratory (Newton *et al.* 2002). Briefly, cryocut coronal sections were subjected to slide-based immunohistochemistry under RNAse-free conditions. Sections were air-dried and then processed for *in-situ* hybridization using radiolabelled riboprobes. Slides were exposed to autoradiographic film to ascertain signal strength and then dipped in emulsion (Kodak, NBT2) for 3 wk. A few slides were test-developed to determine optimal exposure to emulsion.

### In-situ *zymography*

Cryocut rat sections (14 $\mu$m) were allowed to air dry on a rack at room temperature. Gelatin from pig skin, fluorescein conjugate (Invitrogen, USA) was diluted 1:500 in zymography buffer (0.05 M Tris–HCl, 0.15 M NaCl, 5 mM $CaCl_2$). An ImmEdge pen (Vector Laboratories) was used to circumscribe the area around the sections so incubations could be performed directly on slides. Slides were incubated overnight at 37 °C in a foil-covered humid container. The sections were rinsed briefly (1 min) three times in 1 × PBS and fixed in Histochoice tissue fixative (Sigma) at room temperature for 10 min. The slides were rinsed once in 1 × PBS and mounted with Vectashield (Vector Laboratories) and coverslipped. MMP activity was visualized under epifluorescence microscopy (Axiophot; Carl Zeiss, Germany). Images were captured using identical exposure settings for sham and ECS sections.

## Results

### *TIMP-1 and MMP-9 induction in SLM*

Emulsion autoradiography for TIMP-1 showed robust induction in Cresyl Violet-positive cells in SLM after chronic ECS. The grain density was highest in cells that appeared to encircle vasculature, based on the circular pattern of cells expressing TIMP-1 transcript (Fig. 1*a*). The elevation of TIMP-1 mRNA in the SLM region was examined by laser microdissection of Cresyl Violet cells that surrounded the vasculature (Fig. 1*b, c*), followed by real-time PCR analysis. TIMP-1 was induced almost 12-fold and MMP-9 was increased 3-fold (Fig. 1*d*). We investigated the cellular phenotype representation of this region by measuring the expression of specific markers, alpha smooth muscle actin ($\alpha$-SMA), glial fibrillary acidic protein (GFAP), platelet-derived growth-factor receptor beta (PDGFr$\beta$) and platelet endothelial cell adhesion molecule (PECAM/CD31). After normalizing for

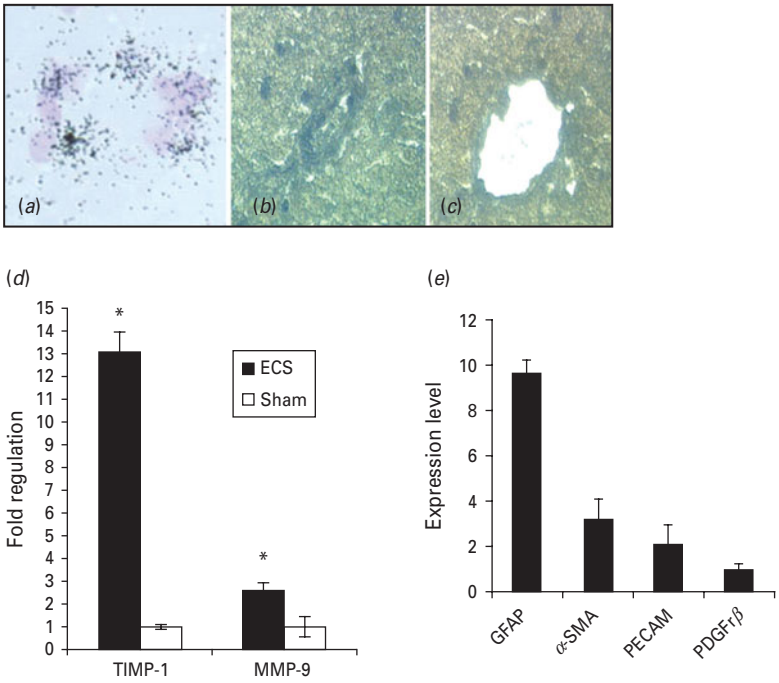


**Fig. 1.** (*a*) The induction of TIMP-1 mRNA in SLM cells is shown by emulsion autoradiography (100× magnification). TIMP-1 (dark grains) is expressed in Cresyl Violet-positive cells (light purple). (*b*) Representative SLM blood-vessel region is shown on PEN foil slide after Cresyl Violet staining, prior to laser microdissection. (*c*) The same vessel after laser microdissection (40× magnification). (*d*) Regulation of TIMP-1 and MMP-9 was measured by real-time PCR in ECS and sham SLM vessels (* $p \leqslant 0.01$, $n = 4$). (*e*) Cell types expressed in microdissected SLM vessels were examined by real-time PCR analysis of representative markers: GFAP, astrocytes; α-SMA, perivascular cells; PDGFrβ, pericytes; PECAM, endothelial cells. Bars represent relative expression levels of the markers ($n = 4$). Amplification cycles at detection threshold: GFAP, 25; α-SMA, 31; PECAM, 32; PDGFrβ, 33.

expression levels of the housekeeping gene *GAPDH*, the relative expression levels of the markers are shown (Fig. 1*e*). These results indicate that the TIMP-1-induced SLM vascular region is composed of multiple cell types, GFAP-positive astrocytes, α-SMA-expressing perivascular cells, PECAM-expressing endothelial cells and PDGFrβ-positive mural cells.

### *TIMP-1 co-localization with MMP-9 and RECA*

TIMP-1 mRNA is maximally regulated after chronic ECS in SLM, GLM and the pial surface of the cortex (Fig. 2*a, b*). Double immunohistochemistry for TIMP-1 and MMP-9 showed both proteins strongly expressed in the same regions (Fig. 2*c, d*). MMP-9 is expressed by both neurons and astrocytes. TIMP-1 protein is expressed at high levels in SLM (Fig. 2*c*) and GLM vessels (Fig. 2*d*). TIMP-1 is observed at a luminal location while MMP-9 appears to be expressed by astrocytes and is abluminal in location. Co-localization of TIMP-1 and MMP-9 is visible as a yellow signal in the area between the luminal and abluminal regions (yellow arrow, Fig. 2*e*). Combined immunohistochemistry and emulsion autoradiography were performed to localize TIMP-1 mRNA with reference to endothelial cells using RECA as a marker for blood vessels. TIMP-1 mRNA expression, evidenced by emulsion grain density, was highest in the vicinity of vasculature (Fig. 2*f, g*) but predominantly co-localized with Cresyl Violet-positive cells rather than RECA-immunostained vessels (Fig. 2*g–i*).

### *MMP-9 co-localization and zymography*

MMP-9 was expressed in the abluminal side of SLM blood vessels and did not co-localize with the luminal endothelial expression of RECA (Fig. 3*a, b*). This could indicate that MMP-9 is expressed in the basement membrane (Fig. 3*b*). ECS-induced MMP-9 expression was seen to co-localize with GFAP-positive astrocytes (Fig. 3*c, d*). A single co-localized cell is shown for clarity in Fig. 3*d*. Only a subset of GFAP cells express MMP-9. This is evident in GLM (inset in Fig. 3*c*) where some GFAP cells are MMP-9 negative and appear to alternate with cells that express both GFAP and MMP-9.

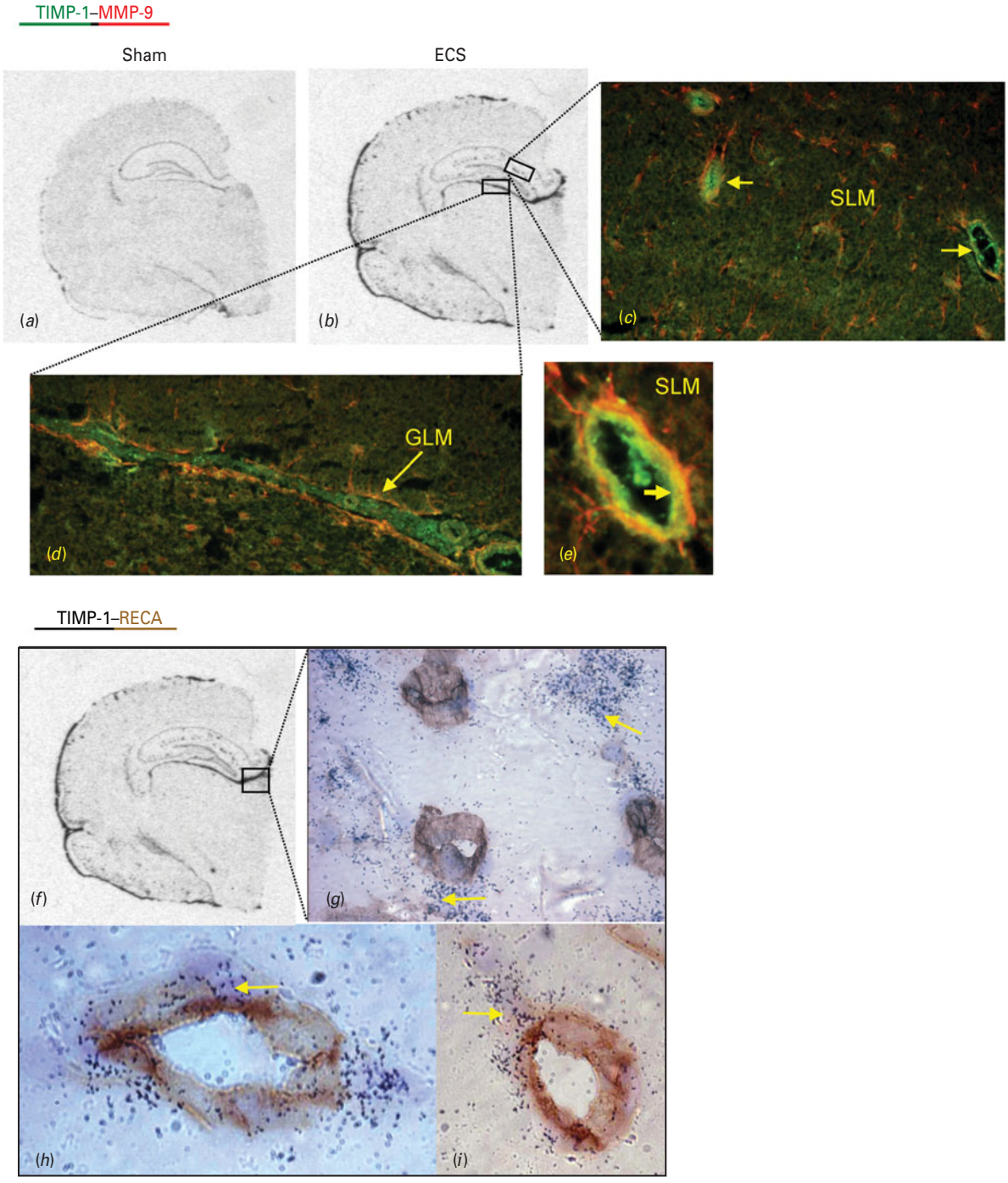


**Fig. 2.** Induction of TIMP-1 in SLM and GLM after chronic ECS is shown in representative sections (*a*, *b*). Double-labelling immunohistochemistry of TIMP-1 (green) and MMP-9 (red) indicates spatial location of protein (yellow arrows) in (*c*) SLM and (*d*) GLM. Both are shown at 40 × magnification. (*e*) Co-localization of TIMP-1 and MMP-9 shown in magnified image of an SLM vessel (100 × magnification), the co-localized region is indicated by yellow arrow. (*f*) ECS-induced TIMP-1 is shown to indicate location of immuno-*in situ* hybridization (*g*–*i*) for RECA protein (brown staining) and TIMP-1 mRNA (dark grains). Cresyl Violet-stained cells expressing TIMP-1 are indicated by black arrows. Vessels are shown at 40 × magnification (*g*). Higher magnification views of SLM vessels are shown in panels (*h*, *i*) (100 × ).

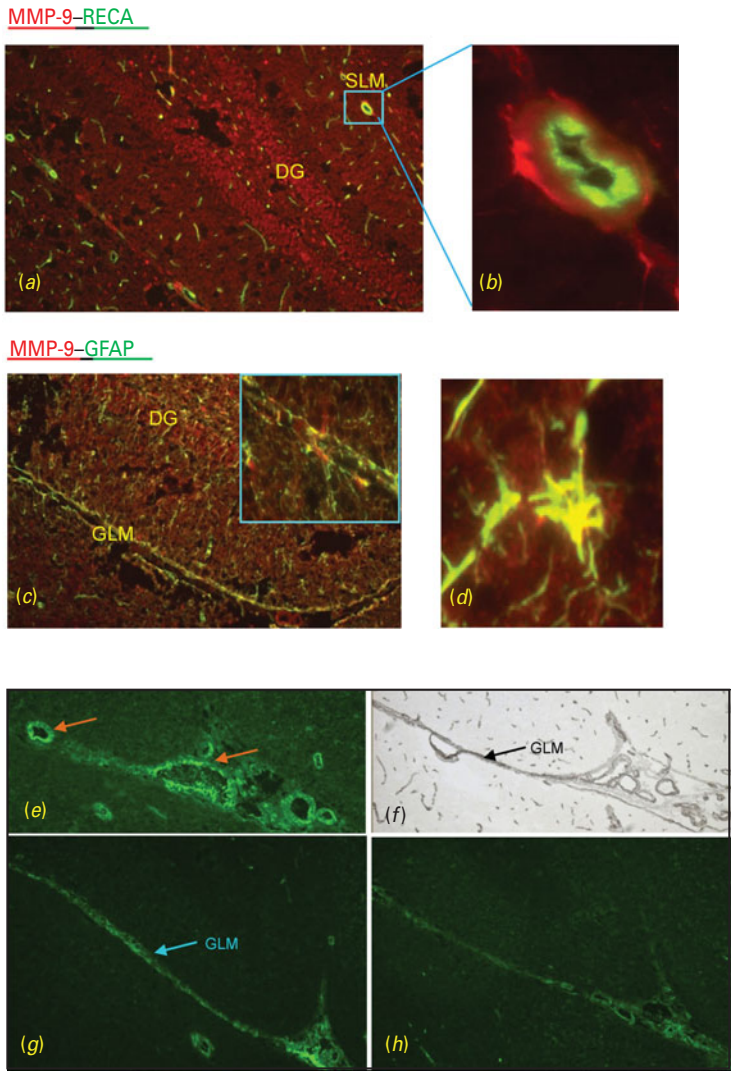


**Fig. 3.** (*a*) Double-labelling immunohistochemistry for MMP-9 (red) and RECA (green) is shown (20× magnification). (*b*) Higher magnification of a single SLM vessel shows abluminal expression of MMP-9 and luminal expression of RECA (100× magnification). (*c*) Double-labelling immunohistochemistry for MMP-9 (red) and GFAP (green) is shown in GLM (100× magnification). A magnified region of GLM is shown as an inset, indicating interspersed co-labelled and independently labelled cells. (*d*) A single co-localized astrocytic cell. Representative sections from *in-situ* zymography for MMP activity in GLM is shown for (*e, g*) ECS and (*h*) sham control. Collagen IV immunostained GLM is shown in panel (*f*) for regional comparison with MMP activity in panel (*e*). Larger vessels are indicated by orange arrows. All images at 20× magnification.

The enzymatic activity of MMP was investigated by *in-situ* zymography using gelatin as the substrate. Higher MMP activity, based on brighter relative fluorescence, was detected in ECS sections (Fig. 3*e, g*) compared to sham control (Fig. 3*h*). Increased MMP activity was restricted to vascular regions of SLM and GLM, with the most pronounced effect in GLM. A collagen IV immunostained section is shown in Fig. 3*f*. Collagen IV is the major structural protein of vascular basement membrane and also the target of MMPs during angiogenesis-associated remodelling.

We employed *in-situ* hybridization analysis with radiolabelled riboprobes to examine the regulation of CTGF after ECS due to its role in remodelling and angiogenesis. CTGF displays a discrete expression pattern restricted to layer 6 of the cortex. ECS strongly induced CTGF (3.5-fold), specifically in the GLM

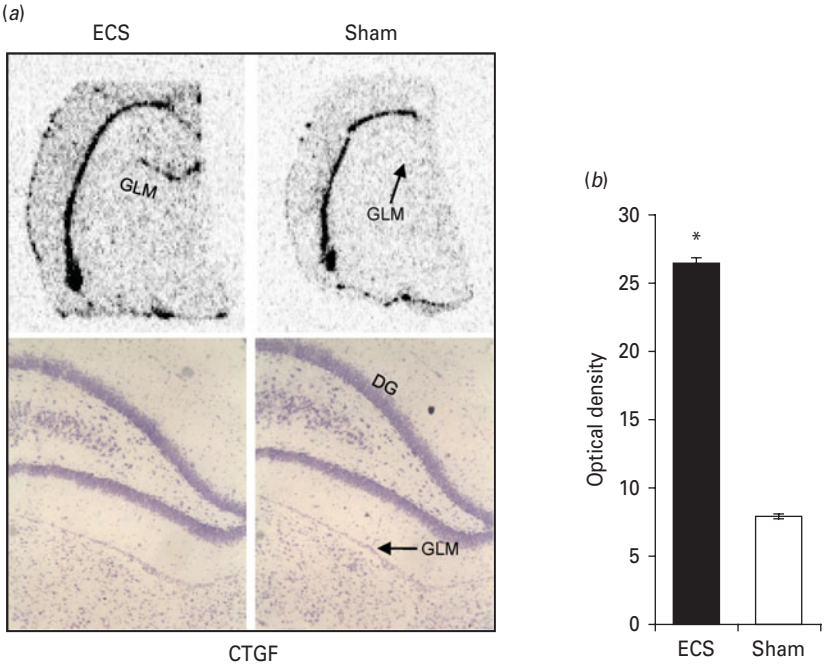


**Fig. 4.** ECS-induced expression of connective tissue growth factor. (*a*) *In-situ* hybridization analysis of CTGF showing specific induction in GLM. Cresyl Violet-stained sections are shown in lower panels for anatomical clarity of GLM. (*b*) Quantified bar graphs of GLM up-regulation ($n = 4$, * $p \leqslant 0.01$).

without any change in basal cortical expression pattern (Fig. 4).

### *Phenotype of TIMP-1 and MMP-9 SLM cells*

The cellular phenotype of TIMP-1- and MMP-9-expressing SLM vascular cells was investigated using laser microdissection combined with single-cell PCR. Sequential images from a SLM vessel microdissection indicating 'before and after' capture images of individual cells (Fig. 4*a*). Of the 20 cells tested, seven were positive for TIMP-1 and four for MMP-9. Each of the TIMP-1 and MMP-9 positive cells were then tested for expression of GFAP, $\alpha$-SMA, PECAM and RGS5. Gel analysis shows the expression of $\alpha$-SMA in cells expressing TIMP-1 and GFAP in cells expressing MMP-9 while other products were not expressed at detectable levels (Fig. 5*b*, *c*).

## Discussion

We have characterized the ECS-induced regulation of TIMP-1 in hippocampal vasculature with a view towards understanding the mechanism of angiogenesis in this region. Previous work by us and others has demonstrated the induction of angiogenic genes (Newton *et al.* 2003), elevation of endothelial proliferation (Hellsten *et al.* 2004) and vascular density (Hellsten *et al.* 2005; Newton *et al.* 2006). Our current results provide support for the involvement of MMP-9 and TIMP-1 in hippocampal vascular remodelling and angiogenesis.

Angiogenic trophic factors such as vascular endothelial growth factor (VEGF) are mainly responsible for the induction of angiogenesis. However, this process includes a supporting cast of molecules and cell types in addition to endothelial cells, functioning in a coordinated series of events. MMPs degrade the basement membrane (BM) (Kalluri, 2003), release matrix-bound trophic factors and assist endothelial cell migration and tubulization (Bergers *et al.* 2000). As endothelial cells bound to BM are usually incapable of proliferation, a localized degradation of BM allows ECs to proliferate and migrate in response to elevation in angiogenic factor activity. The increase in ECS-induced MMP-9 activity in the hippocampus, indicated by gene induction and zymography, occurs mainly at sites that are invested with larger vessels. As the major component of BMs is collagen IV (LeBleu *et al.* 2007), it is useful to note that MMP activity coincides with regions (GLM and SLM) that exhibit strong collagen IV expression (Newton *et al.* 2006).

While MMPs have well-defined functional involvement in angiogenesis, their powerful membrane-digesting actions can damage the extracellular matrix.

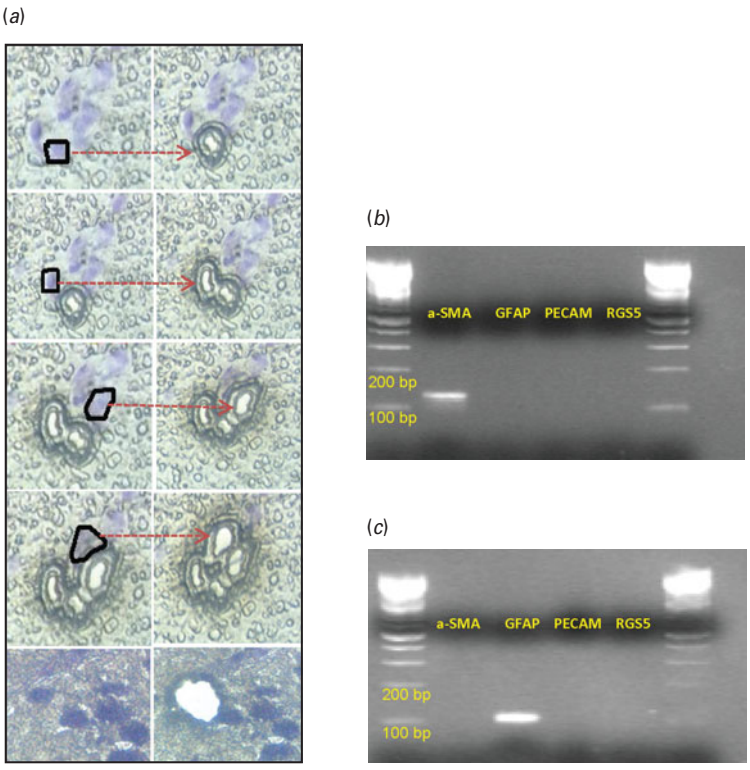


**Fig. 5.** Cellular phenotype of TIMP-1- and MMP-9-expressing cells. (*a*) Serial images of SLM cell laser microdissection. Individual cells were outlined with free draw tools (left panels) and excised for collection (right panels). A single Cresyl Violet cell is shown before and after excision in the bottom panel. TIMP-1- and MMP-9-positive cells were identified by real-time PCR analysis. cDNA of cells positive for (*b*) TIMP-1 or (*c*) MMP-9 were subjected to real-time PCR detection for $\alpha$-SMA, GFAP, PECAM and RGS5 and the products analysed by gel electrophoresis with molecular-weight markers. Amplification cycles to detection threshold : TIMP-1, 31 ; MMP-9, 35.

This is kept in check by the activity of a specific class of inhibitors, i.e. TMIPs. Of the four known TIMPs 1–4, only TIMP-1 is highly induced by ECS (Newton *et al.* 2003). TIMP-1 specifically neutralizes MMP-9, the most abundant brain MMP. The increase in MMP activity by ECS appears to be restricted to vascular BMs, serving as an angiogenic stimulus and facilitating vascular remodelling. The level of MMP induction with ECS is modest compared to pathological conditions (Deryugina & Quigley, 2006) and neurodegeneration models (Jourquin *et al.* 2003). Although MMP elevation has been mostly associated with pathological changes and neurodegenerative damage, it is interesting to note that the late-phase of stroke recovery requires MMP-9 functional activity and suppression of MMP inhibited remodelling and therapeutic neovascularization (Zhao *et al.* 2006). Genetic or pharmacological suppression of ECS-induced TIMP-1 could reveal the importance of precisely regulating MMP activity and provide insight into the balance between physiological and pathological remodelling.

It is intriguing to note that the induction of TIMP-1 and MMP-9 can exhibit significant variability in cellular phenotype based on insult and pathological state (Muir *et al.* 2002). TIMP-1 was specifically induced in the granular layer of the dentate gyrus after acute ECS, but shifts to the molecular layer after chronic ECS (Newton *et al.* 2003). Understanding the relationship between dentate gyrus *vs.* SLM expression as a function of ECS treatments is a topic for further study. A limitation of our approach is that we have examined only acute and chronic treatments. It will be useful to investigate intermediate time-points for regional TIMP-1 induction and also determine the time-course of MMP-9 elevation. Future studies could also investigate additional cell types (e.g. oligodendrocytes, NG-2), not addressed in this study, as potential sources of TIMP1 expression.

CTGF has been implicated in multiple physiological and pathological events. The initial understanding that CTGF is primarily involved in fibrosis has undergone significant revision as numerous studies

have shed light on the multi-functionality of this trophic factor (Moussad & Brigstock, 2000). The role of CTGF in neovascularization has been demonstrated by *in-vitro* and *in-vivo* angiogenesis assays (Shimo *et al.* 1999). CTGF knockout mice studies showed that expression of extracellular matrix remodelling genes and VEGF was reduced in the absence of CTGF (Ivkovic *et al.* 2003). Predominantly induced by TGF$\beta$1, CTGF has several distinct protein domains that serve to interact with a wide variety of functionally different proteins, including PDGF, TGF$\beta$1, integrins and MMPs. It appears that CTGF couples matrix remodelling with angiogenesis by interacting with molecules involved in both processes (Rundhaug, 2005; Shimo *et al.* 1999). It is therefore interesting to note that CTGF is elevated in the same region (GLM) where MMP is active. However, further work is required to understand whether this anatomical overlap is due to physical interaction of the molecules. As vascular remodelling occurs in concert with angiogenesis, a regulatory molecule capable of mediating the actions of angiogenic factors and matrix proteins could play a pivotal role in controlling the spatial aspects of neovascularization.

The SLM is a metabolically active region and a major site of glucose utilization in the hippocampus in response to memory tasks (Sybirska *et al.* 2000) and ketamine stimulation (Duncan *et al.* 2003). As glucose in the brain is delivered via blood vessels, the SLM vessels are likely to be significantly involved in meeting the needs of increased metabolic activity in the hippocampus. Remodelling to support angiogenesis could occur in response to metabolic demands or cues from increased blood flow through SLM vessels. The therapeutic efficacy of ECS could also be related to an increase in brain microcirculation, resulting in improved humoral, trophic and oxygenation support to neurons. The elevation in angiogenic factors (that are frequently also neurotrophic) could positively influence the neurovascular unit, leading to improved brain function. Further work could be directed at examining the neurovascular unit in other models with antidepressant efficacy such as physical exercise.

### Acknowledgements

This work was supported by National Institute of Health Grants nos. MH072894-01 (S.S.N.) and U24NS051869-01 (S.S.N.).

### Statement of Interest

None.

### References

**Altar CA, Laeng P, Jurata LW, Brockman JA, *et al.*** (2004). Electroconvulsive seizures regulate gene expression of distinct neurotrophic signaling pathways. *Journal of Neuroscience* **24**, 2667–2677.

**Bergers G, Brekken R, McMahon G, Vu TH, *et al.*** (2000). Matrix metalloproteinase-9 triggers the angiogenic switch during carcinogenesis. *Nature Cell Biology* **2**, 737–744.

**Deryugina EI, Quigley JP** (2006). Matrix metalloproteinases and tumor metastasis. *Cancer Metastasis Review* **25**, 9–34.

**Duncan GE, Miyamoto S, Lieberman JA** (2003). Chronic administration of haloperidol and olanzapine attenuates ketamine-induced brain metabolic activation. *Journal of Pharmacology and Experimental Therapeutics* **305**, 999–1005.

**Hellsten J, Wennstrom M, Bengzon J, Mohapel P, *et al.*** (2004). Electroconvulsive seizures induce endothelial cell proliferation in adult rat hippocampus. *Biological Psychiatry* **55**, 420–427.

**Hellsten J, West MJ, Arvidsson A, Ekstrand J, *et al.*** (2005). Electroconvulsive seizures induce angiogenesis in adult rat hippocampus. *Biological Psychiatry* **58**, 871–878.

**Ivkovic S, Yoon BS, Popoff SN, Safadi FF, *et al.*** (2003). Connective tissue growth factor coordinates chondrogenesis and angiogenesis during skeletal development. *Development* **130**, 2779–2791.

**Jourquin J, Tremblay E, Decanis N, Charton G, *et al.*** (2003). Neuronal activity-dependent increase of net matrix metalloproteinase activity is associated with MMP-9 neurotoxicity after kainate. *European Journal of Neuroscience* **18**, 1507–1517.

**Kalluri R** (2003). Basement membranes: structure, assembly and role in tumour angiogenesis. *Nature Reviews Cancer* **3**, 422–433.

**LeBleu VS, Macdonald B, Kalluri R** (2007). Structure and function of basement membranes. *Experimental Biology and Medicine* (*Maywood*) **232**, 1121–1129.

**Madsen TM, Treschow A, Bengzon J, Bolwig TG, *et al.*** (2000). Increased neurogenesis in a model of electroconvulsive therapy. *Biological Psychiatry* **47**, 1043–1049.

**Malberg JE, Eisch AJ, Nestler EJ, Duman RS** (2000). Chronic antidepressant treatment increases neurogenesis in adult rat hippocampus. *Journal of Neuroscience* **20**, 9104–9110.

**Moussad EE, Brigstock DR** (2000). Connective tissue growth factor: what's in a name? *Molecular Genetics and Metabolism* **71**, 276–292.

**Muir EM, Adcock KH, Morgenstern DA, Clayton R, *et al.*** (2002). Matrix metalloproteases and their inhibitors are produced by overlapping populations of activated astrocytes. *Brain Research. Molecular Brain Research* **100**, 103–117.

**Newton SS, Collier EF, Bennett AH, Russell DS, *et al.*** (2004). Regulation of growth factor receptor bound 2 by electroconvulsive seizure. *Brain Research. Molecular Brain Research* **129**, 185–188.

**Newton SS, Collier EF, Hunsberger J, Adams D, *et al.*** (2003). Gene profile of electroconvulsive seizures: induction of

neurotrophic and angiogenic factors. *Journal of Neuroscience* **23**, 10841–10851.

**Newton SS, Dow A, Terwilliger R, Duman R** (2002). A simplified method for combined immunohistochemistry and in-situ hybridization in fresh-frozen, cryocut mouse brain sections. *Brain Research. Brain Research Protocols* **9**, 214–219.

**Newton SS, Girgenti MJ, Collier EF, Duman RS** (2006). Electroconvulsive seizure increases adult hippocampal angiogenesis in rats. *European Journal of Neuroscience* **24**, 819–828.

**Nibuya M, Morinobu S, Duman RS** (1995). Regulation of BDNF and trkB mRNA in rat brain by chronic electroconvulsive seizure and antidepressant drug treatments. *Journal of Neuroscience* **15**, 7539–7547.

**Rundhaug JE** (2005). Matrix metalloproteinases and angiogenesis. *Journal of Cellular and Molecular Medicine* **9**, 267–285.

**Shimo T, Nakanishi T, Nishida T, Asano M, *et al.*** (1999). Connective tissue growth factor induces the proliferation, migration, and tube formation of vascular endothelial cells in vitro, and angiogenesis in vivo. *Journal of Biochemistry* **126**, 137–145.

**Sybirska E, Davachi L, Goldman-Rakic PS** (2000). Prominence of direct entorhinal-CA1 pathway activation in sensorimotor and cognitive tasks revealed by 2-DG functional mapping in nonhuman primate. *Journal of Neuroscience* **20**, 5827–5834.

**Zhao BQ, Wang S, Kim HY, Storrie H, *et al.*** (2006). Role of matrix metalloproteinases in delayed cortical responses after stroke. *Nature Medicine* **12**, 441–445.